Supplementary Figures

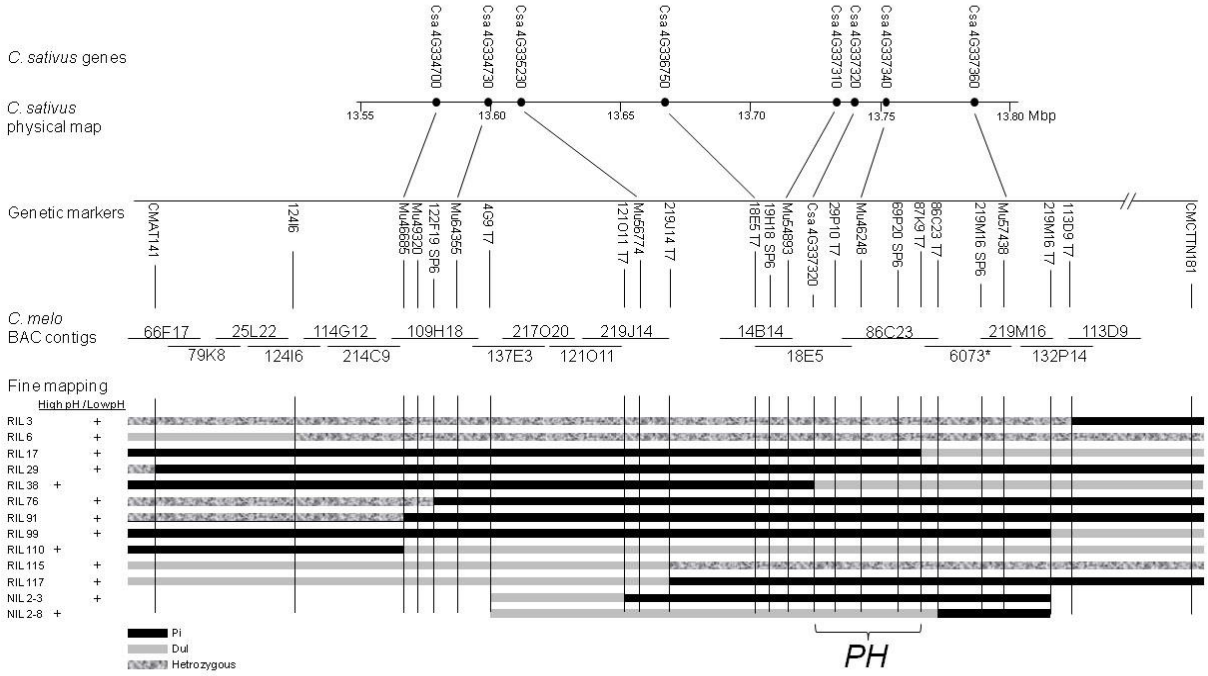

Supplementary Fig. 1. Synteny between *C. sativus* and *C. melo* used for BAC contig determination and fine-mapping of *C. melo PH* gene. Genes and genetic markers of a ~ 0.25 Mbp segment of a *C. sativus* physical map showing synteny with a *C. melo* interval containing the *PH* locus flanked by two SSR markers. *C. melo* BACs were used for contig construction and MAP based cloning as described in the Methods section. Fine mapping of this segment shows sour and non-sour RIL and NIL *C. melo* genotypes flanking the *PH* locus. Sour and non-sour genotypes are indicated in black and grey bars (respectively), and hetrozygous (sour) genotypes are indicated in mottled bars. *, 6073 is a *C. sativus* contig.

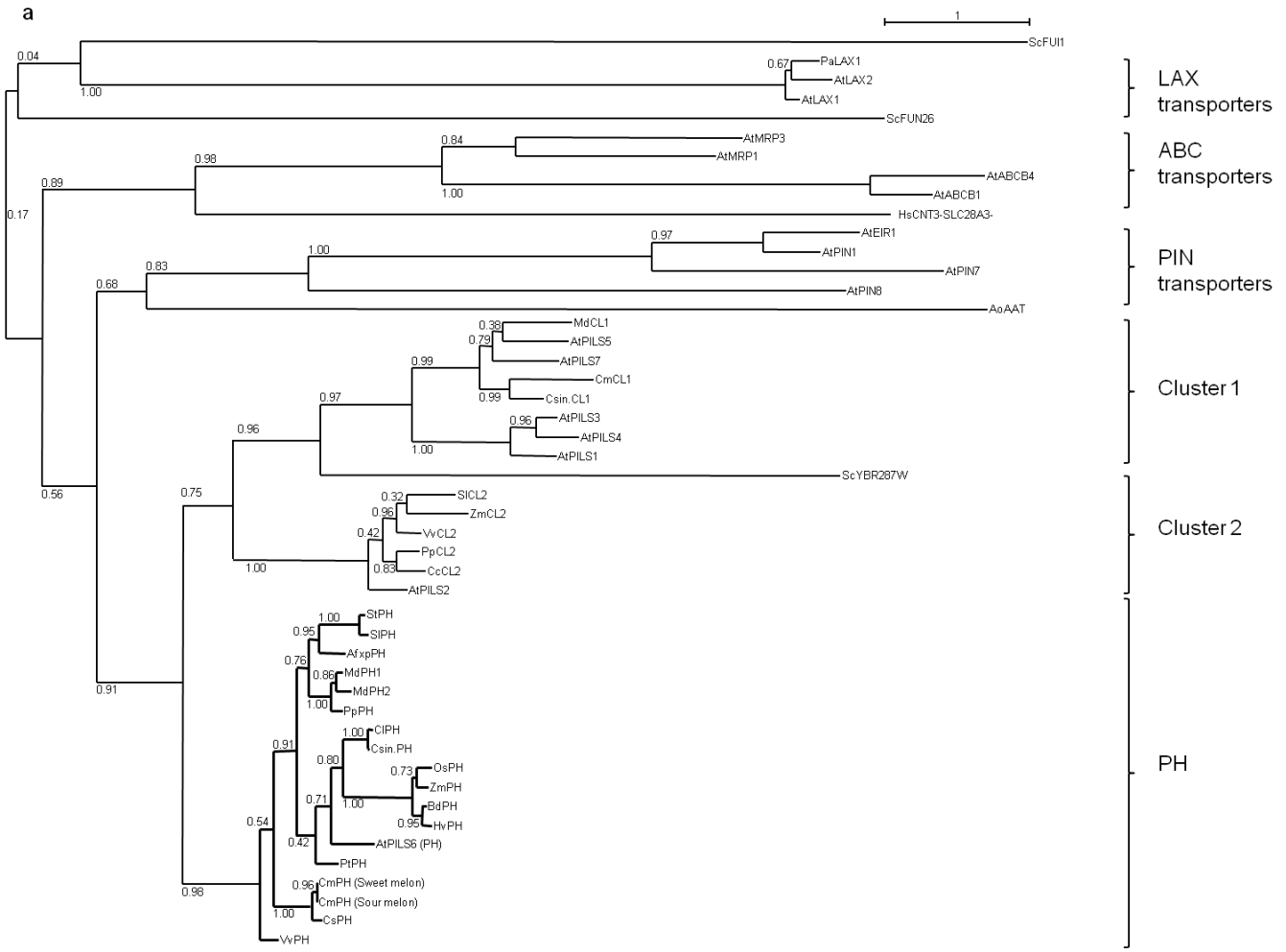
a
1
ScFUI1
0.04
0.67
PaLAX1
AtLAX2
AtLAX1
1.00
ScFUN26
LAX transporters
0.84
AtMRP3
AtMRP1
0.98
AtABCB4
0.89
1.00
AtABCB1
0.17
HsCNT3-SLC28A3-
ABC transporters
0.97
AtEIR1
1.00
AtPIN1
AtPIN7
0.83
0.68
AtPIN8
AoAAT
PIN transporters
0.38
MdCL1
0.79
AtPILS5
0.99
AtPILS7
CmCL1
0.99
Csin.CL1
0.97
0.96
AtPILS3
1.00
AtPILS4
AtPILS1
ScYBR287W
Cluster 1
0.56
0.75
0.32
SlCL2
0.96
ZmCL2
0.42
VvCL2
PpCL2
1.00
0.83
CcCL2
AtPILS2
Cluster 2
1.00
StPH
0.95
SlPH
AfxpPH
0.76
0.86
MdPH1
MdPH2
0.91
1.00
PpPH
1.00
ClPH
0.91
Csin.PH
0.80
0.73
OsPH
ZmPH
0.71
1.00
BdPH
0.95
HvPH
0.54
0.42
AtPILS6 (PH)
PtPH
0.98
0.96
CmPH (Sweet melon)
CmPH (Sour melon)
1.00
CsPH
VvPH
PH

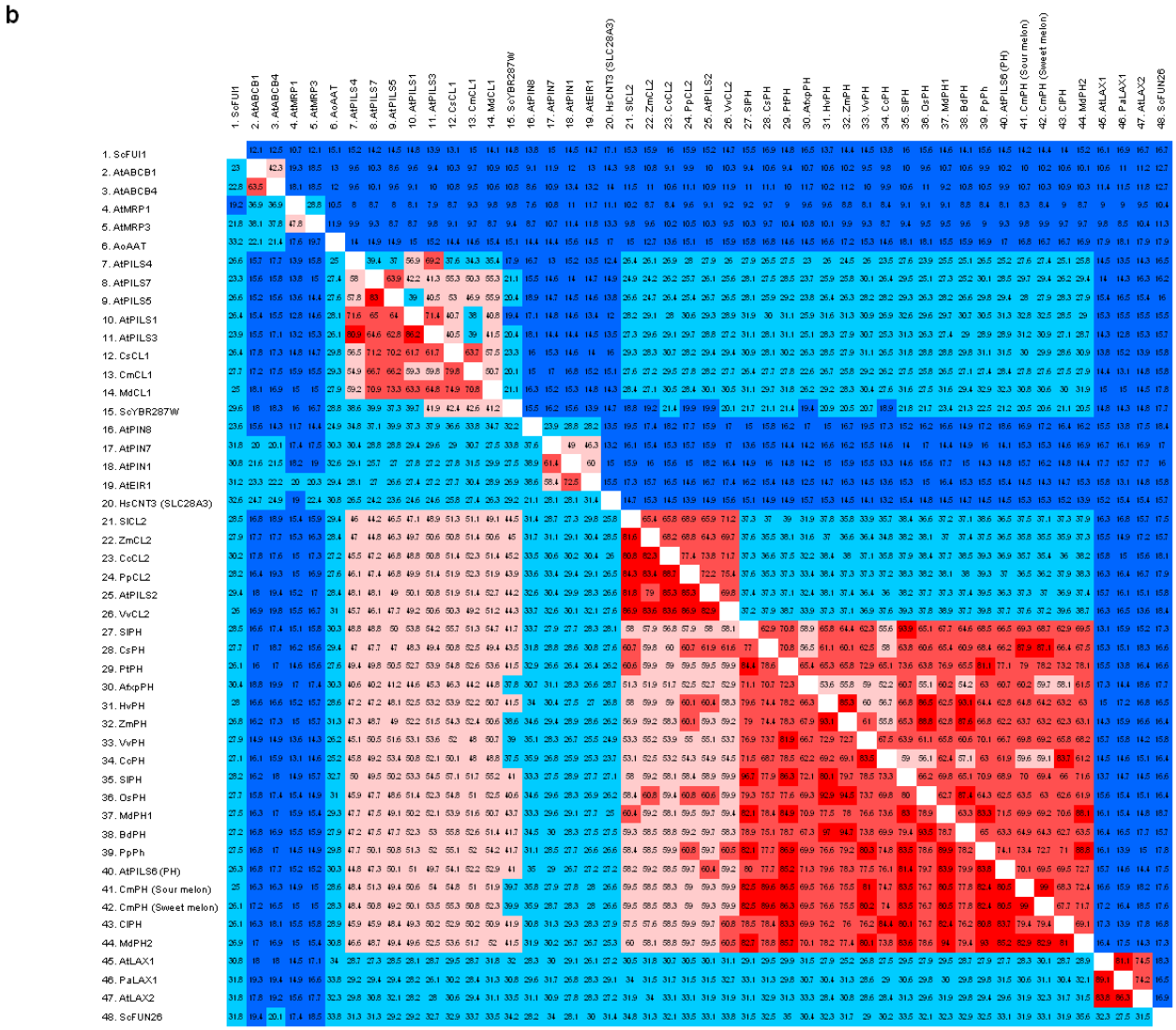

Supplementary Fig. 2. A clade of enzymes acting as pH regulators in the large plant transporter protein family. (**a**) The full length protein sequences were aligned and phylogenetic tree was built as described in Methods. The approximate likelihood ratio test (aLRT) Shimodaira-Hasegawa-like (SH-like) procedure was used as a statistical test to calculate branch support. aLRT statistical values are displayed at the tree nodes. The tree branches corresponding to the PH proteins are marked in bold. The accession numbers of the proteins used for the preparation of this tree and the organism names are listed in Supplementary table S1. (**b**) Similarity and identity pairwise matrix of the 48 proteins used for generation of the phylogenetic tree in (a) was calculated using MatGAT 2.02 (http://bitincka.com/ledion/matgat/) run with BLOSUM62. In the lower left side the percentage of similarity is presented, whereas in the upper right side of the figure is presented the percentage of identity between the proteins.

Supplementary Fig. 3. Schematic representation of transmembrane prediction for the *PH* gene. The red lines indicate a putative transmembrane domain suggested by each of the prediction programs (17 programs, see Supplementary methods). Blue squares indicate 10 amino acids. Detailed figure presented in Supplementary Data 1.

a

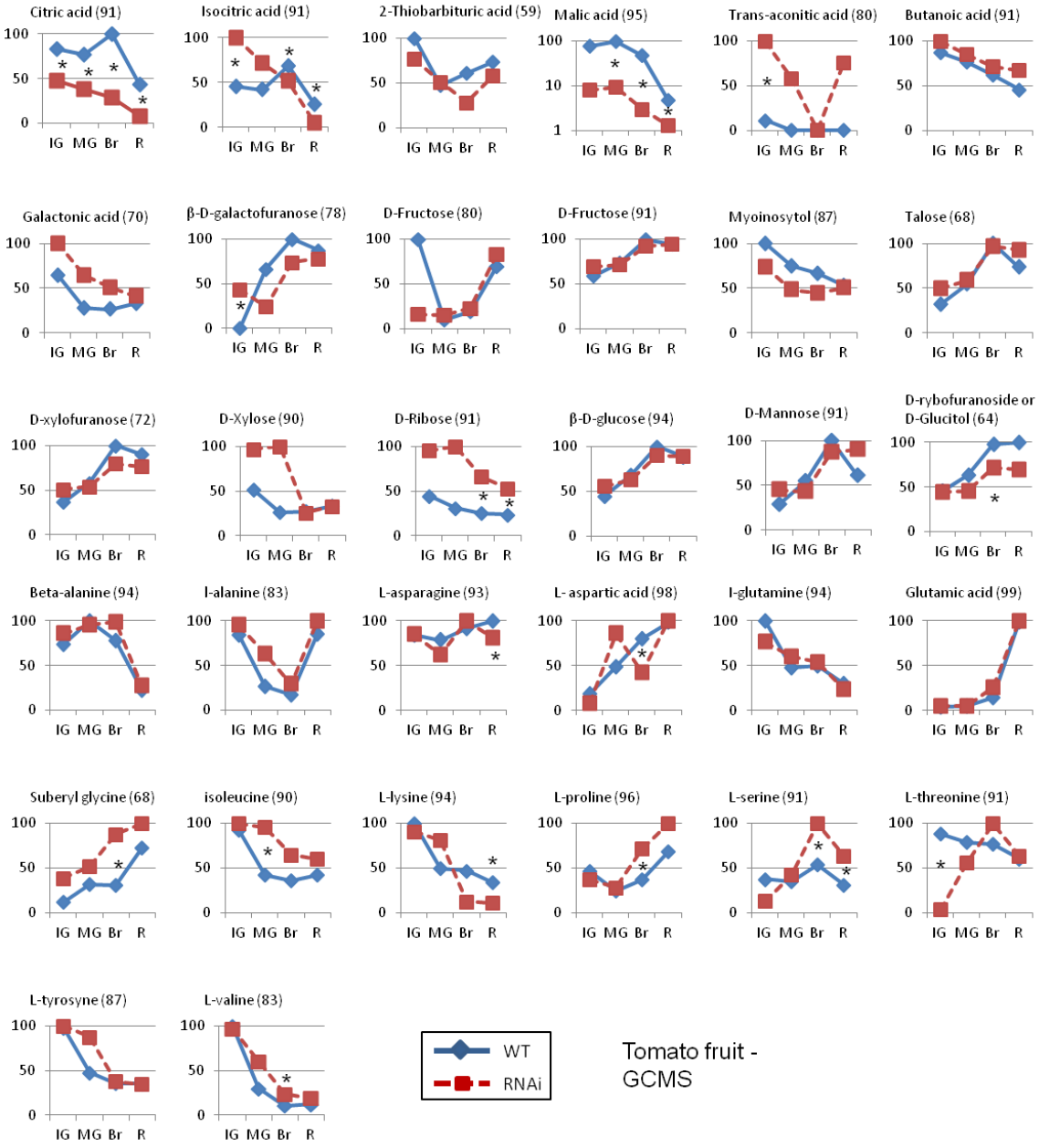
Citric acid (91)
Isocitric acid (91)
2-Thiobarbituric acid (59)
Malic acid (95)
Trans-aconitic acid (80)
Butanoic acid (91)
Galactonic acid (70)
β-D-galactofuranose (78)
D-Fructose (80)
D-Fructose (91)
Myoinosytol (87)
Talose (68)
D-xylofuranose (72)
D-Xylose (90)
D-Ribose (91)
β-D-glucose (94)
D-Mannose (91)
D-rybofuranoside or D-Glucitol (64)
Beta-alanine (94)
l-alanine (83)
L-asparagine (93)
L- aspartic acid (98)
l-glutamine (94)
Glutamic acid (99)
Suberyl glycine (68)
isoleucine (90)
L-lysine (94)
L-proline (96)
L-serine (91)
L-threonine (91)
L-tyrosyne (87)
L-valine (83)
IG MG Br R
WT
RNAi
Tomato fruit - GCMS

b

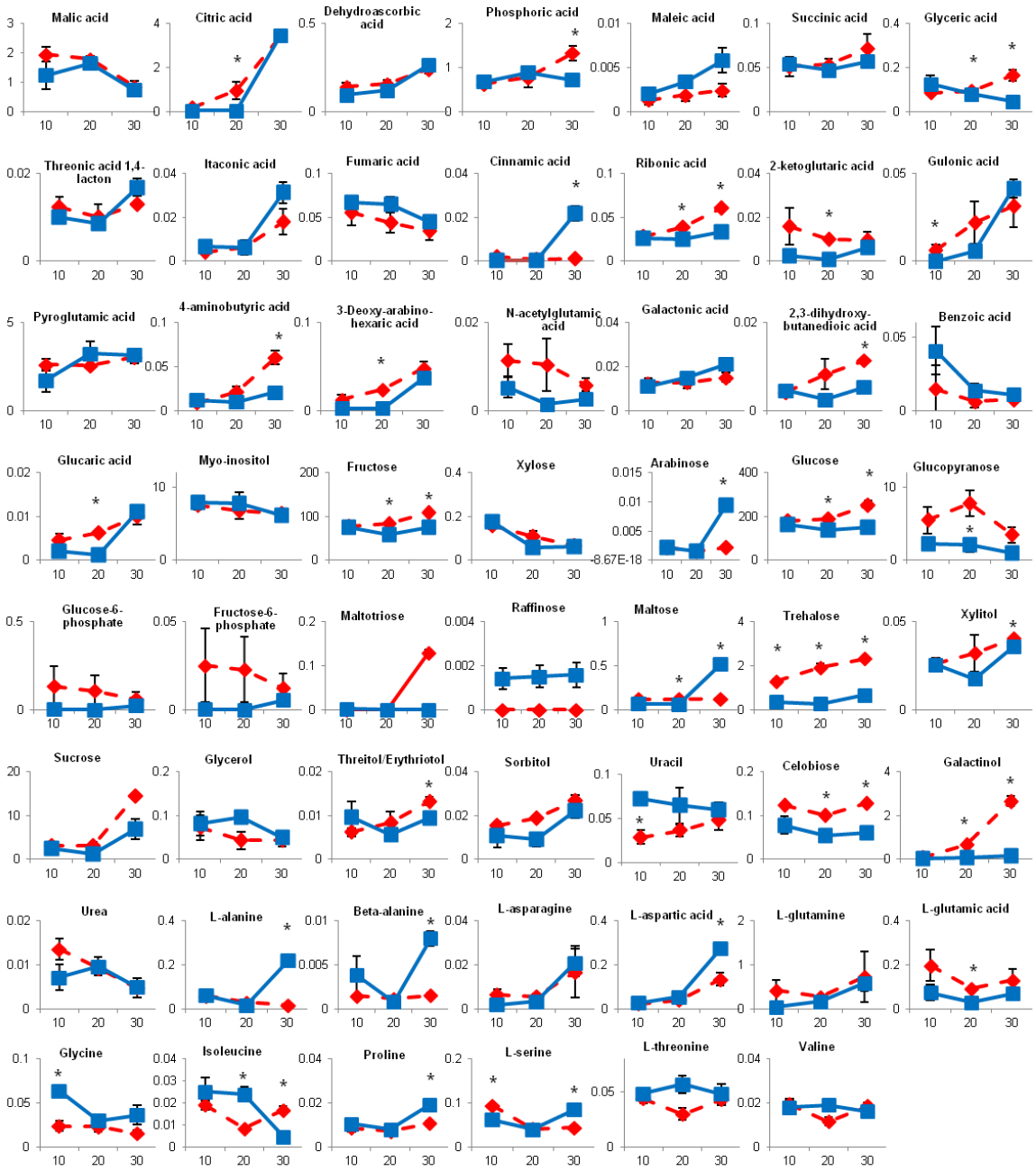

Melon fruit - GCMS

Sour (PI414723)

Non-sour (Dulce)

Supplementary Fig. 4. Changes in the levels of several metabolites throughout the development of tomato and melon fruit. GC-MS was performed following derivatization of tissue extracts from fruit throughout development of (**a**) transgenic silenced and non-silenced tomato fruit and (**b**) melon fruit from sour (PI414723) and non-sour (Dulce) parental lines of the RILs population. Student's *t*-test results for significance ($P < 0.05$; $n = 3$) are indicated by an asterisk. Numbers in parentheses in (a) represent score given by Chemstation™ program (Agilent technologies) to putative metabolite. The scale in (a) is normalized to 100% and the scale in (b) represents peak areas.

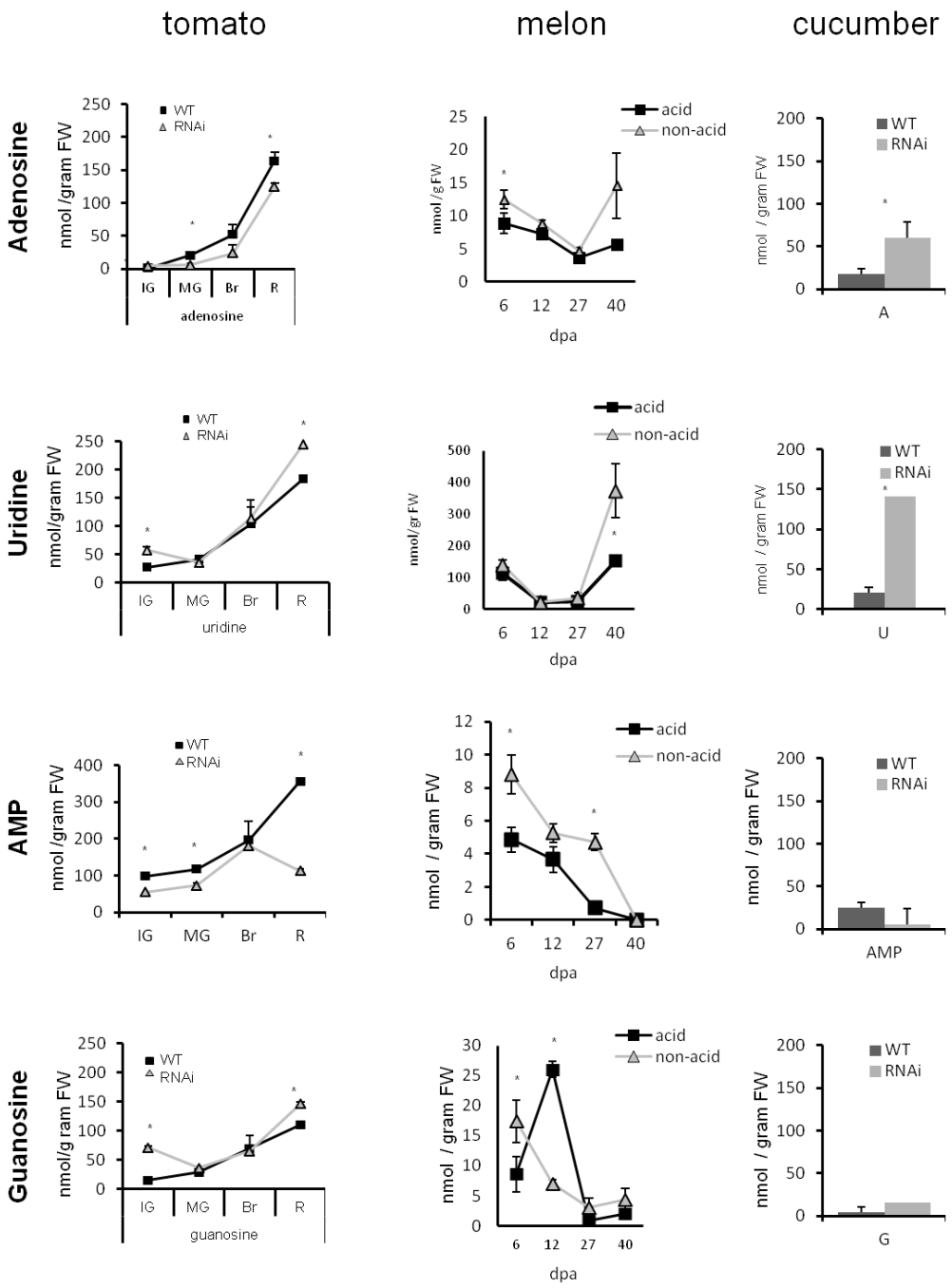

Supplementary Fig. 5. Values of uridine, adenosine, guanosine and AMP in tomato and melon fruit through development and in ripe cucumber fruit. Tomato and cucumber fruit are from the transgenic silenced and non-silenced genotypes (T_1) and the data for melon are derived from the near-isogenic melon genotypes. Student's t-test results for significance ($P < 0.05$; n = 3) are marked with an asterisk. FW, fresh weight; IG, immature green; MG, mature green; Br, breaker; R, red; FW, fresh weight; dpa, days post anthesis. Error bars are SEM of three biological replicates.

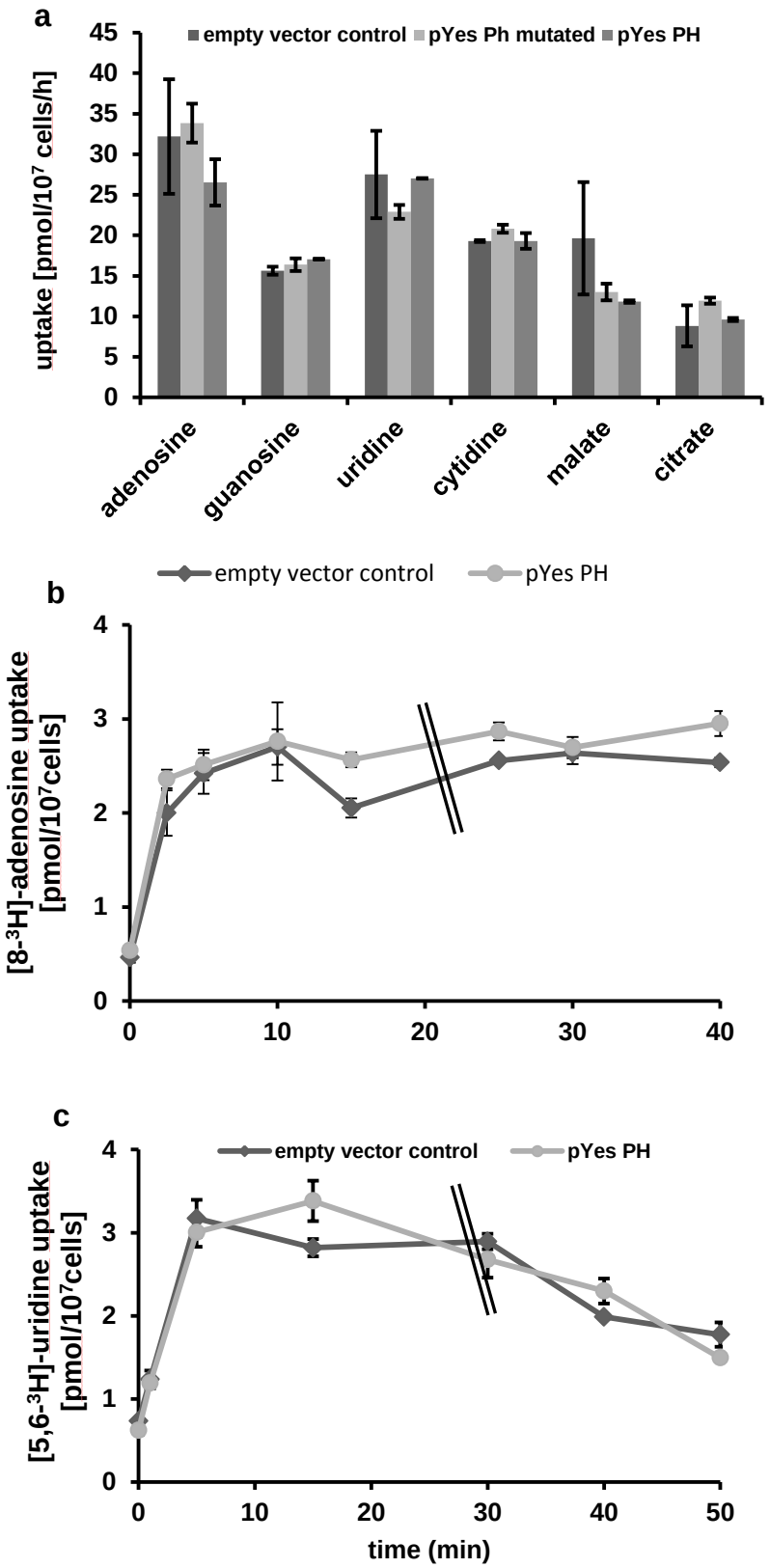

Supplementary Fig. 6. (**a**) Uptake of nucleosides and organic acids after incubating yeast cells for 5 min. at 30°C in sodium phosphate buffer containing 200µM triciated nucleosides and [^{14}C-] radioactive labeled malic and citric acid respectively. After washing three times with sodium-phosphate buffer, filters were transferred to scintillation tubes and radioactivity on the filters was quantified by liquid-scintillation counting in a Tri-Carb 2810 TR scintillation counter (PerkinElmer). The mutated PH gene contains the four amino acid duplication (Dulce type). (**b**) Adenosine uptake and subsequent exudation measured in yeast cells. Time-dependent uptake of [8-^{3}H]-adenosine [100µM] for up to 20 min. Cells were afterwards centrifuged for 30 sec. at 11.000g and then washed with fresh sodium-phosphate buffer without adenosine to measure potential exudation of radioactive substrate out of the cells. (**c**) Uridine uptake and subsequent exudation measured in yeast cells. Time-dependent uptake of [5,6-$_{3}$H]-uridine [100µM] for up to 30 min. Cells were afterwards centrifuged for 30 sec at 11.000g and then washed with fresh sodium-phosphate buffer without uridine to measure potential exudation of radioactive substrate out of the cells.

a

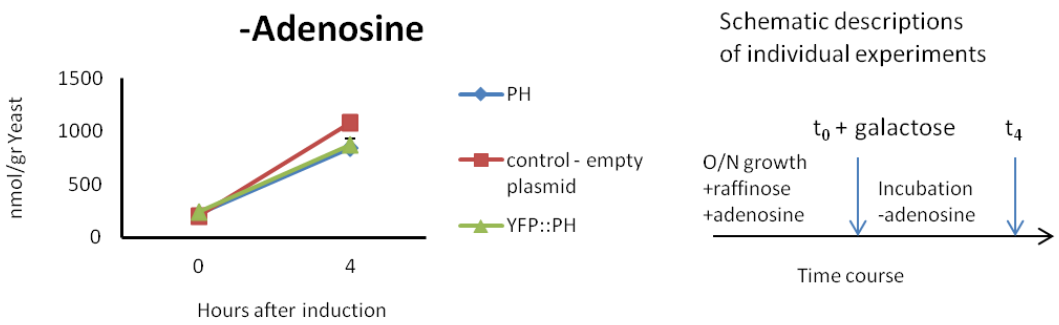
-Adenosine
nmol/gr Yeast
1500
1000
500
0
0
4
Hours after induction
PH
control - empty plasmid
YFP::PH
Schematic descriptions of individual experiments
t0 + galactose
t4
O/N growth
+raffinose
+adenosine
Incubation
-adenosine
Time course

b

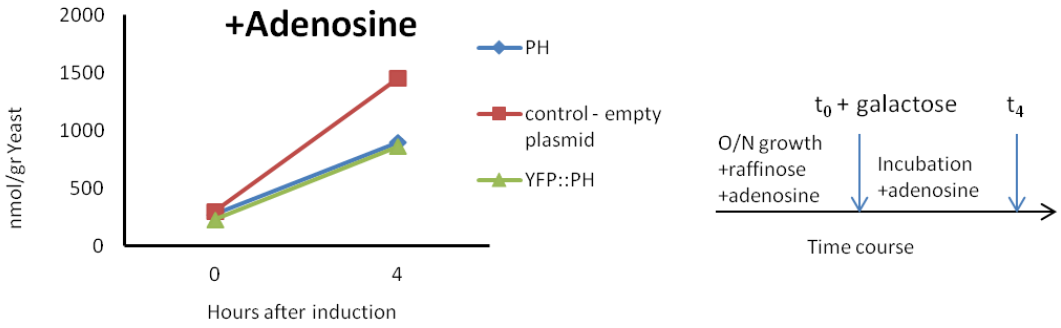
+Adenosine
nmol/gr Yeast
2000
1500
1000
500
0
0
4
Hours after induction
PH
control - empty plasmid
YFP::PH
t0 + galactose
t4
O/N growth
+raffinose
+adenosine
Incubation
+adenosine
Time course

c

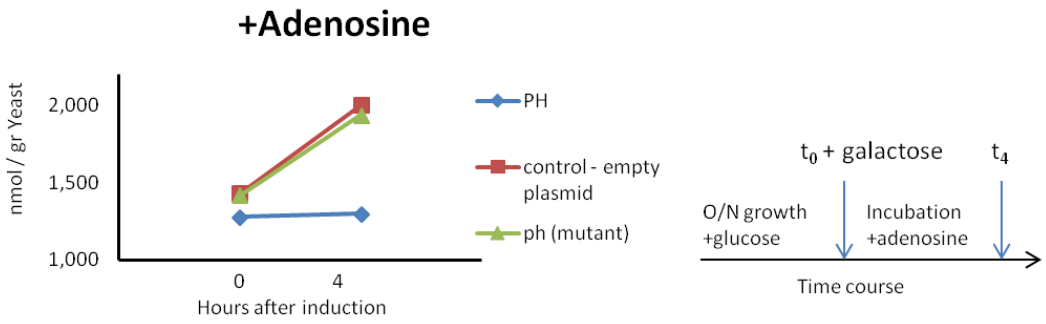
+Adenosine
nmol / gr Yeast
2,000
1,500
1,000
0
4
Hours after induction
PH
control - empty plasmid
ph (mutant)
t0 + galactose
t4
O/N growth
+glucose
Incubation
+adenosine
Time course

d

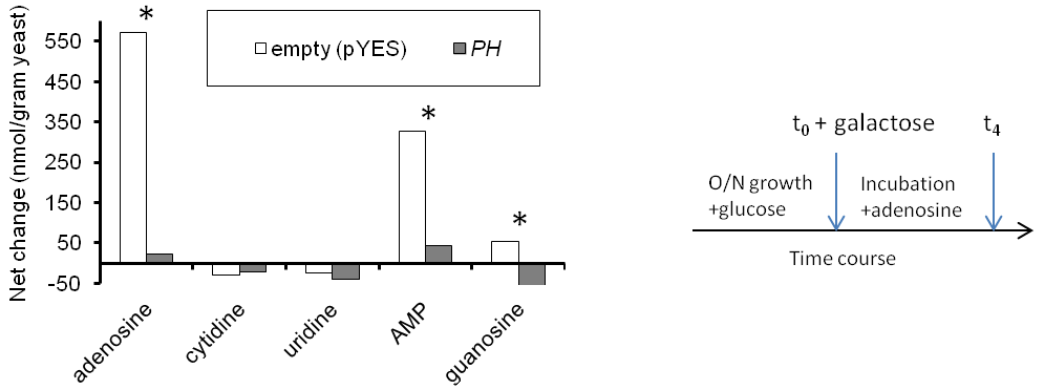
Net change (nmol/gram yeast)
550
450
350
250
150
50
-50
empty (pYES)
PH
*
*
*
adenosine
cytidine
uridine
AMP
guanosine
t0 + galactose
t4
O/N growth
+glucose
Incubation
+adenosine
Time course

Supplementary Fig. 7. Effect of Adenosine feeding on Adenosine content of Yeast. Nucleosides were measured at t_0 following overnight (O/N) growth in either raffinose (**a, b**) or glucose (**c, d**) with adenosine, and again following four hours incubation under galactose without (**a**) or with (**b, c, d**) addition of adenosine, as described in the methods section. The methods for the individual experiments are presented in schematic form. (**a, b**) show the increase in endogenous adenosine content during 4 hr incubation and the reduction in increase due to the *PH* gene. The YFP::PH construct (shown localized to the ER in Fig. 3) causes the same reduction as the PH gene alone, indicating function at the ER localization. The reduction in increase during the 4 hr incubation is seen also in the absence of exogenous adenosine, suggesting that the effect of the *PH* gene is not directly on transport but rather indirectly affecting nucleoside homeostasis. (**c**) Adenosine levels in yeast in response to the *PH* gene and the mutant *PH* gene (Dulce type containing the 4-amino acid duplication) indicates that the duplication leads to dysfunction of the gene, and adenosine increase is identical in both the empty plasmid control and the mutant PH gene. (**d**) An additional experiment showing the difference in net change in nucleosides of yeast following four hours incubation and indicate increase in adenosine together with AMP, as well as smaller differences in guanosine. Data are expressed as net change during the adenosine feeding period (t_{4h}-t_0). Student's t-test results for significance ($P < 0.05$; $n = 3$) are marked with an asterisk.

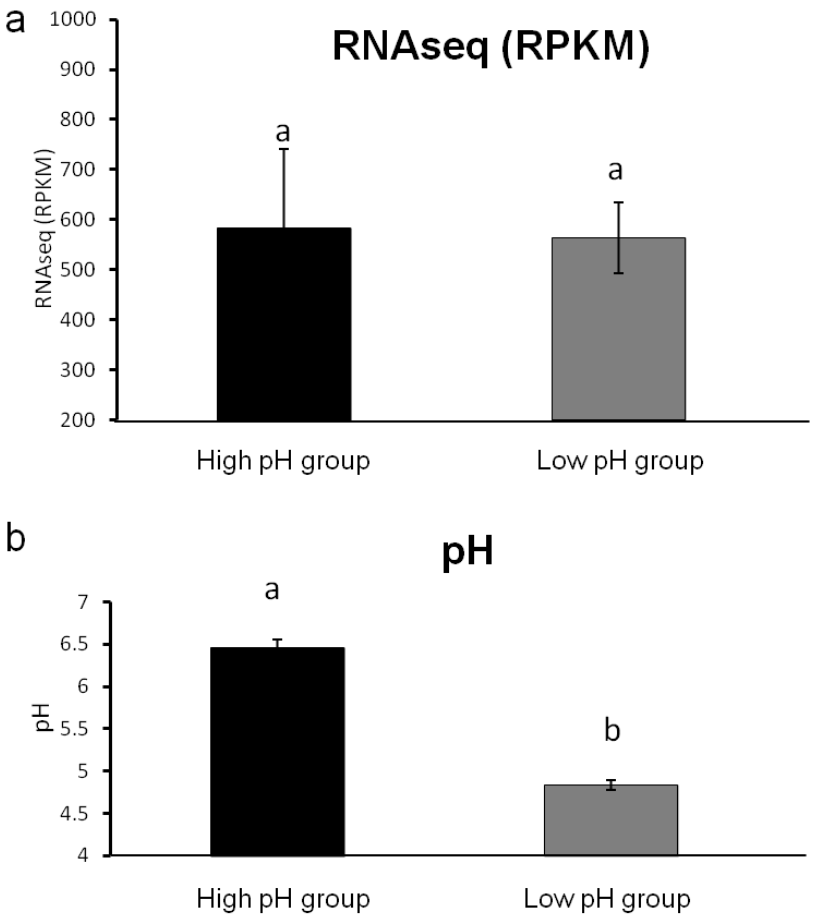

Supplementary Fig. 8. *PH* gene expression in low and high pH lines. (**a**) Mean expression (RPKM) of *PH* gene MELO3C025264 of 24 RILs with the 11 highest and 13 lowest pH values in fruit flesh at the mature stage. Data is based on expression analysis (RNA-seq) based on fruit from five pooled biological samples for each line. (**b**) Mean pH values of mature fruits from the same lines, performed on the same fruit samples of the RNA-seq experiment. Different letters indicate significant differences (p-value < 0.05) between averages of group lines (High pH and Low pH), according Tukey-Kramer HSD test.

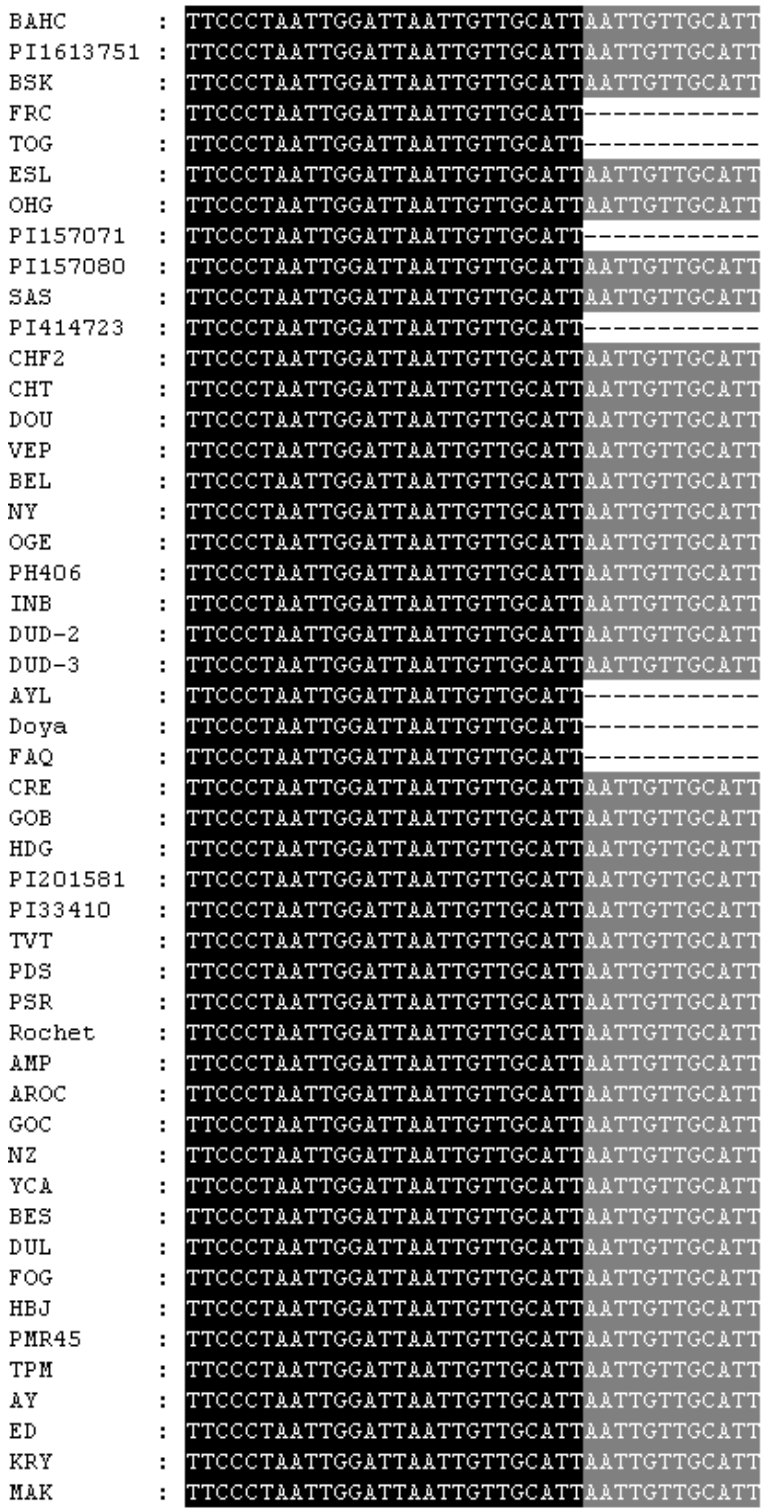

Supplementary Fig. 9. Alignment of the DNA sequences coding for the LIGLIVA and LIGLIVALIVA amino acid sequences of the 3rd TMD of the *C. melo PH* gene. Primers used for sequencing are described in Supplementary table S3. The seven accessions with gaps (FRC, TOG, PI157071, PI414723, AYL, Doya and FAQ; described in Supplementary data 6) have low pH fruit flesh. The remaining accessions all have high pH fruit flesh and have the identical 12bp duplicated sequence.

Melon Gene	Cucumber ortholog	Annotation	Expression in melon	Expression tissue	No. ESTs
MELO3C025262	Csa4G337320	none	not detected		0
MELO3C025263	Csa4G337330	Similar to E3 ubiquitin-protein ligase RING1 (Gossypium hirsutum) (uniprot_sprot:sp|P0CH30|RING1_GOSHI)	MU47918	cotyledon CMV infected	1
				root healthy (Pinyonet torpedo)	2
			MU67454	Vedrantais callus	1
			MU65296	root infected (Pinyonet torpedo)	1
MELO3C025264	Csa4G337340	Similar to Auxin:hydrogen symporter, putative (Ricinus communis) (uniref90:UniRef90_B9T0P6)	MU46248	T-111 fruit (15DAP)	1
				cotyledon CMV infected	3
				mature fruit (Noy Yizre'el)	1
				root healthy (Pinyonet torpedo)	1
				root infected (Pinyonet torpedo)	1
MELO3C025265	Csa4G337350	none	not detected		0

Supplementary Table 1. Expression of four candidate genes in melon tissues determined from fine mapping. Expression data is taken from the ICUGI public database (www.icugi.org) and gene sequences are derived from the Melonome database (http://melonomics.net/). Fruit expression is colored yellow.

Primer name	Forward sequence 5'-3'	Reverse sequence 5'-3'
CMAT141	CCACCCGTAACCAGAGGACTAA	GAGGGATAACATGTCCATTAGA
CMCTTN181	CTCTCTGCAATTCTCGCC	CAACCATCCGCTTCACTC
4G9 T7	GGGTGGTTTTCTTTCTGACTA	CCCTGTTCGGTAAAGTCAGT
121O11 T7	CACCGTGTATCTGGAGATCT	CAGGCTCCCCTGAATTGTAT
69P20 SP6	GGCCTTATGTGATGGATGCT	CACCGCACAAATCCGTAGAT
29P10 T7	GGAGCACTGTTCCAACCTT	GCTGGGTTGAAGGTAAAGGA
87K9 T7	CAAATGATGAGTGTAAGCTATGA	CATAGCTTACACTCATCATTTGA
86C23 T7	CTCCACTTCCATGGTACCATT	CCAGTGTAGGACTCTTGTTT
219M16 SP6	CAACAGGAAAATGAGTTCAGATA	GCCGACATCATCTCGTTTCTA
219M16 T7	CACCACAATTTGCCTACTTA	CCCACTCACC AGACACTTTT
113D9 SP6	CTACCACTTTTGGTCCTTGAA	CCACATGTGAATGTTTGAGGA
122F19 SP6	CGACCCAGTTCCATGATCTA	GGCGAGGGCAAATTTAATGT
219J14 T7	GCCGAATAGAGCCTAAGAT	ATGATTTTAGGGAGAGATT
18E5 T7	CCTGCGGATGTATCTGAAGA	CCCGCTTGAACCTACAACA
109H18 SP6	GACAGCGACTACGACGAAA	GTCAGGGTCGTGGAATGTAT
MU46685	GCGCCTTTGAACTCGAAGAA	CCCACATGCTTCATTCATATAT
MU49320	CCGTTGCATCGTCACTACAA	CTGGGAGGATATCAACATTTAAA
MU46248	CCACCCTGCCATTGAGATGA	GGGAGGAAACCTCGTTGAA
MU64355	GCTCTATTCGGTTTCTTTACA	GCAGGCGATGGAGAAGGTAA
MU56774	GGGAGGCTTTCAGTTGGAT	CGGGATCTACCAGCAGAAAT
MU54893	GACCGGACTGTACTTAACTT	CCTCTTGAACATCGACCGTTT
MU57438	CTACCTGTTTCCTACTCCAAA	CCCGCCACTACATCCGAAAA
Csa4G337320	GAGGAGACAAGCAATCACCA	GGAGGAACAACAGGAAGAACT
19H18 SP6	GACGATTTTAGGAGATGATATAA	GGCTTGTACTCCACGTACTT
MU65008	GCGTCACTTCGCACTTCAGA	CCAGTGAAGGGCGTTAAGTT
MELO3025262	GCCATATGCGATCCAAGAGT	CTGGCTACGGTTTGAGGTAT
C. melo PH (full length)	ATGGACATGGAAAGATTTCTCT	TTAGAAGAGTATCCTGAAGTAGA
S. lycopersicum PH (full length)	ATGGATAGGGTGTCGAGGAT	TTAAAAGAGTATGTTGAGGTAGA
pGA580-CmPH	TCTAGAATGGACATGGAAAGATTTCTCT	AGATCTGGGAATTCGATTTTAGAAGAGT
pGA580-SlPH	TCTAGAATGGATAGGGTGTCGAGGAT	AGATCTGCGGGAATTCGATTTTAAAAGA
RNAi-CmPH	CTCGAGTCTAGACCAGTGGGTTGGTGCAATTA	GGTACCATCGATCGGCTAACATGACTATGCCA
RNAi -SlPH	CTCGAGTCTAGACAGCCGACTCTAGTAGTTCA	GGTACCATCGATCCATCCAGCCATAGAGATCA
CmPH-yeast	GGGGACAAGTTTGTACAAAAAAGCAGGCTATGGACATGGAAAGATTTCTCT	GGGGACCACTTTGTACAAGAAAGCTGGGTTTAGAAGAGTATCCTGAAGTAGAGGA
YFP-SlPH	GGGGACAAGTTTGTACAAAAAAGCAGGCTATGGTGAGCAAGGGCGAGGA	GGGGACCACTTTGTACAAGAAAGCTGGGTTTAAAAGAGTATGTTGAGGTAGA

Supplementary Table 2. Primers used

Name	Accession number	Species name
AfxpPH	TC29778	*Aquilegia formosa x pubescens*
AoAAT	XP_001817113.2	*Aspergillus oryzae RIB40*
AtABCB1	AEC09320.1	*Arabidopsis thaliana*
AtABCB4	NP_182223.1	*Arabidopsis thaliana*
AtEIR1	NP_568848.1	*Arabidopsis thaliana*
AtLAX1	AED90315.1	*Arabidopsis thaliana*
AtLAX2	AEC07116.1	*Arabidopsis thaliana*
AtMRP1	AEE31212.1	*Arabidopsis thaliana*
AtMRP3	NP_850575.1	*Arabidopsis thaliana*
AtPILS1	NP_683316.1	*Arabidopsis thaliana*
AtPILS2	NP_565011.1	*Arabidopsis thaliana*
AtPILS3	NP_565133.1	*Arabidopsis thaliana*
AtPILS4	NP_177779.1	*Arabidopsis thaliana*
AtPILS5	NP_565417.1	*Arabidopsis thaliana*
AtPILS6 (PH)	NP_195819.1	*Arabidopsis thaliana*
AtPILS7	NP_201399.1	*Arabidopsis thaliana*
AtPIN1	Q9C6B8.1	*Arabidopsis thaliana*
AtPIN7	AEE30333.1	*Arabidopsis thaliana*
AtPIN8	NP_197157.4	*Arabidopsis thaliana*
BdPH	XP_003564484.1	*Brachypodium distachyon*
CvPH	WMU09803	*Citrullus vulgaris*
CsiCL2	orange1.1g012968m	*Citrus sinensis*
CsiPH	orange1.1g016799m	*Citrus sinensis*
ClPH	UC52_39795	*Citrus limon*
CmCL1	MELO3C013710	*Cucumis melo*
CmPH (Sower)	MU46248	*Cucumis melo*
CmPH (Sweet)	MU46248	*Cucumis melo*
CsCL1	Csa3M000690	*Cucumis sativus*
CsPH	Csa01116	*Cucumis sativus*
CpPH	PU053110	*Cucurbita pepo*
HsCNT3(SLC28A3)	NP_071410.1	*Homo sapiens*
HvPH	AK251406	*Hordeum vulgare*
MdCL1	MDP0000225382	*Malus domestica*
MdPH1	MDP0000162143	*Malus domestica*
MDPH2	*MDP0000298711*	*Malus domestica*
OsPH	NP_001044627.1	*Oryza sativa*
PaLAX1	CAI05895.1	*Prunus avium*
PpCL2	ppa002140m	*Prunus persica*
PpPH	ppa006224m	*Prunus persica*
PtPH	EEF05451	*Populus trichocarpa*
ScFUN26	P31381.1	*Saccharomyces cerevisiae*
ScYBR287W	gi51012631	*Saccharomyces cerevisiae*
Sc FUI1	CAA84862.1	*Saccharomyces cerevisiae*
SlCL2	Solyc02g091240.1.1	*Solanum lycopersicum*
SlPH	Solyc10g074790.1.1	*Solanum lycopersicum*
StPH	PGSC0003DMP400048171	*Solanum tuberosum*
VvCL2	GSVIVP00022326001	*Vitis vinifera*
VvPH	GSVIVT00033630001	*Vitis vinifera*
ZmCL2	NP_001148375.1	*Zea mays*
ZmPH	AFK32351.1	*Zea mays*

Supplementary Table 3. Accession numbers of the sequences used for the construction of the phylogenetic tree and the protein identity/similarity pairwise matrix (Supplementary Fig. 2).

Supplementary Methods

Stable *Agrobacterium*-mediated plant transformation.

All pGreen vectors were introduced into electro-competent *Agrobacterium tumefaciens* 'EHA105' cells harboring the pSOUP helper plasmid[1] via electroporation.

Cucumber. Cucumber RNAi stable transformation was carried out using the described melon RNAi vector pGreen-RNAi-*CmPH* in the 'Ilan' variety (Zeraim Gedera Co., Gedera, Israel; http://www.zeraim.com) using procedures previously described[2]. As the variety is parthenocarpic and monoecious, the variety 'Derby' (Hishtil Co., Ashqelon, Israel; http://www.hishtil.com) was used as pollinator.

Tomato. Tomato transformations of RNAi pGreen-RNAi-*SlPH*, pGreen-*YFP-SlPH* and pGreen-*SlPH-GFP* constructs were carried out in the described 'MP1' tomato line[3] using procedures previously described[4].

Tobacco. The described pGreen-*YFP-SlPH* vector's stable transformation into tobacco was carried out using procedures previously described[5].

Microscopy and cellular localization.

Organellar localization of the *PH* gene was determined in yeast, melon fruit and various tobacco organs, including protoplasts, as described above. The analysis was performed by comparing the fluorescence imaging of a transiently expressed fluorescent (RFP) organelle marker harboring the ER targeting sequence HDEL[6] and that of the YFP or GFP (N-terminal and C-terminal, respectively) fused tomato *PH* gene.

Fluorescence Imaging. Observation of fluorescently labeled cells was preformed via an Olympus IX81/FV500 (Japan) laser-scanning microscope. The GFP channel was used in order to observe GFP or YFP florescence (via settings of 488 nm excitation and BA505-525 emission filter). Observation of RFP florescence was preformed via settings of 543

nm excitation and BA610 emission filter. When more than one color (GFP, YFP and RFP) was monitored in the same sample, a DM (dichroic mirror) 488/543 was used, and sequential acquisition was performed. Chlorophyll auto-fluorescence was determined as light above 660 nm. Confocal optical sections were obtained at 0.5 µm increments. 3D images were obtained using the FLUOVIEW 500 software supplied with the CLSM. Transmitted light images were obtained using Nomarski differential interference contrast (DIC). Manual microscopy images of yeast in figure S4 (F and G) were obtained using an Olympus IX71 microscope controlled by the Delta Vision SoftWoRx 3.5.1 software with ×60 oil lens. Images were captured by a Photometrics Coolsnap HQ camera with excitation at 490/20 nm and emission at 528/38 nm (GFP). Images were transferred to Adobe Photoshop CS3 for slight contrast and brightness adjustments.

Tissue sampling for metabolic profiling.

For HPLC, fresh or frozen (-80^{o}C) fruit tissue was ground in liquid nitrogen using IKA A11 grinder. Then 600ul of methanol: water (1:1) was added to 200 mg fine ground powder and the resulting mixture was vortexed for 30 seconds, sonicated for 15 min and vortexed again for 30 seconds. The sample was cleaned of debris by centrifugation (20,000g) and by filtration using Axiva syringe filters (PTFE, 0.2 µm). For GCMS analysis fruit tissue was prepared as described previously[7].

HPLC-DAD. The analysis was carried out on an Agilent 1200 HPLC system with an Agilent 1200 Diode Array Detector (DAD). The analytical columns used were: Zorbax Stable Bond - C18 column (4.6x150.0 mm, 5.0 µm, Agilent Technologies, USA). The mobile phase contained A, H2O with 0.1% formic acid; B, 100% HPLC grade acetonitrile. The column was equilibrated with 100% A, and then the sample was injected, reaching 50% B gradient after 25 min. The mobile phase flow was 1.0 ml min^{-1}. Each substance was identified by co-migration with commercial standards and by matching the spectrum of each nucleoside peak against that of a standard.

Adsorbosphere Nucleotide-Nucleoside column (4.6x250mm, 7µm, Alltech Associates, Deerfield, USA). The mobile phase contained A, H2O with 0.1% formic acid; B, 100%

HPLC grade methanol. The column was equilibrated with 95% A and 5% B, and then the sample was injected, reaching 50% B gradient after 15 min. The mobile phase flow was 1.5 ml min^{-1}. Each nucleoside was identified by co-migration with commercial standards and by matching the spectrum of each nucleoside peak against that of a standard.

HPLC-MS. The analysis was carried out on an Agilent 1290 Infinity series liquid chromatograph coupled with an Agilent 1290 Infinity DAD and Agilent 6224 Accurate Mass Time of Flight (TOF) mass spectrometer (MS). The analytical column was: Zorbax Extend-C18 Rapid Resolution HT column (2.1x50.0 mm, 1.8 μm, Agilent Technologies, Waldbronn, Germany) Mass spectrometry was performed using an Agilent 6224 Accurate Mass TOF LC/MS System equipped with a dual-sprayer orthogonal ESI source, with one sprayer for analytical flow and one for the reference compound (Agilent Technologies, Santa Clara, USA). The mobile phase contained A, H2O with 0.1% formic acid; B, 100% HPLC grade acetonitrile. The column was equilibrated with 100% A, and then the sample was injected, reaching 50% B gradient after 10 min. The mobile phase flow was 0.4 ml min^{-1}. Each substance was identified by co-migration with commercial standards and by matching the mass spectrum of putative peak against that of a standard. The chromatogram was initially analyzed by MassHunter Qualitative Analysis software v.B.05.00 (Agilent) and further analyzed by MassHunter Mass Profiler software v.B.05.00 (Agilent).

GC-MS. GC-MS analysis of derivatized melon extracts and the analysis of the GC-MS data was done as described previously[8]. The GC-MS analysis of derivatized tomato extracts was performed as follows: a 1.0 μl aliquot of the sample was injected into an Agilent GC-MS 6890/5973N system (CA, USA). The instrument was equipped with Rxi-5sil MS column (30.0 m length × 0.25 mm i.d., 0.25 μm film thickness, stationary phase 95% dimethyl- 5% diphenyl polysiloxane). Helium (9.46 psi) was used as a carrier gas with split (1:100) injection. The injector temperature was 330°C, and the detector temperature was 300°C. The following conditions were used: initial temperature 45°C for

1 min, followed by a ramp of 15°C min^{-1} to 105°C, then 5°C min^{-1} up to 215°C followed by 5°C min^{-1} up to 320°C (5 min). A quadrupole mass detector with electron ionization at 70 eV was used to acquire the MS data in the range of 40 to 600 m/z. MS Quad was set to 150°C, MS Source was set to 240°C and MSD Transfer Line Heater was set to 300°C. A

mixture of straight-chain alkanes (C7-C23) was injected into the column under the above-mentioned conditions for determination of retention indices. The identification of the volatiles was assigned by comparison of their retention indices with those of literature and by comparison of spectral data with standard or with the Nist 98 and QuadLib 2205 GC-MS libraries.

Protein transmembrane domain modeling

Transmembrane prediction was performed with the following programs using default parameters unless otherwise noted: DAS TMfilter[9], HMMTOP[10], MemBrain[11], Minnou[12], MEMSAT[13], MEMSAT-SVM[14], oreinTM (pred-tmr2)[15], PHD[16], Philius[17], Phobius[18], SOSUI[19], Split 4.0[20], SVMTM[21], TMHMM[22], Tmpred[23], TOPCONS[24] and Toppred (-e, Kyte-Doolittle hydropathy)[25].

Supplementary References

1. K. Edwards, C. Johnstone, C. Thompson, A simple and rapid method for the preparation of plant genomic DNA for PCR analysis. *Nucleic Acids Res* **19,** 1349 (1991).
2. M. Petreikov, Shen S, Yeselson Y, Levin I, Bar M, Schaffer AA. Temporally extended gene expression of the ADP-Glc pyrophosphorylase large subunit (AgpL1) leads to increased enzyme activity in developing tomato fruit. *Planta* **224,** 1465 (2006).
3. R. P. Hellens, E. A. Edwards, N. R. Leyland, S. Bean, P. M. Mullineaux, pGreen: a versatile and flexible binary Ti vector for *Agrobacterium*-mediated plant transformation. *Plant Mol. Biol.* **42,** 819 (2000).
4. S. McCormick, Transformation of tomato with *Agrobacterium tumefaciens*. In Plant Tissue Culture Manual: Fundamentals and Applications, K. Lindsey, ed (Dordrecht, The Netherlands: Kluwer Academic Publishers), 1 (1991).
5. R.B Horsch, Fry, J. E. Hoffmann, N. L. Eichholtz, D. Rogers, S. G. Fraley, R. T., A simple and general method for transferring genes into plants. *Science* **227,** 1229 (1985).

6. Y.L. Liu, M. Schiff, S.P. Dinesh-Kumar, Virus-induced gene silencing in tomato. *Plant J.* **31,** 777 (2002).
7. B.K. Nelson, X. Cai, A. Nebenführ, A multi-color set of in vivo organelle markers for colocalization studies in *Arabidopsis* and other plants. *Plant J.* **51**, 1126 (2007).
8. M. Itkin, I. Rogachev, N. Alkan, T. Rosenberg, S. Malitsky, L. Masini, S. Meir, Y. Iijima, K. Aoki, R. de Vos, D. Prusky, S. Burdman, J. Beekwilder and A. Aharoni. GLYCOALKALOID METABOLISM1 is required for steroidal alkaloid glycosylation and prevention of phytotoxicity in tomato. *Plant Cell.* **23**, 4507. (2011).
9. M. Cserzo, F. Eisenhaber, B. Eisenhaber, and I. Simon. On filtering false positive transmembrane protein predictions. *Protein Eng* **15**, 745-752 (2002).
10. G.E. Tusnady, and I. Simon. The HMMTOP transmembrane topology prediction server. *Bioinformatics* **17**, 849-850 (2001).
11. H. Shen, and J.J. Chou. MemBrain: Improving the Accuracy of Predicting Transmembrane Helices. *PLoS One* **3**, e2399 (2008).
12. B. Cao, A. Porollo, R. Adamczak, M. Jarrell, and J. Meller. Enhanced recognition of protein transmembrane domains with prediction-based structural profiles. *Bioinformatics* **22**, 303-309 (2006).
13. D.T. Jones. Improving the accuracy of transmembrane protein topology prediction using evolutionary information. *Bioinformatics* **23**, 538-544 (2007).
14. T. Nugent, and D.T. Jones. Transmembrane protein topology prediction using support vector machines. *BMC Bioinformatics* **10**, 159 (2009).
15. C. Pasquier, and S.J. Hamodrakas. An hierarchical artificial neural network system for the classification of transmembrane proteins. *Protein Eng* **12**, 631-634 (1999).
16. B. Rost. PHD: predicting one-dimensional protein structure by profile-based neural networks. *Methods Enzymol* **266,** 525-539 (1996).
17. S.M. Reynolds, L. Kall, M.E. Riffle, J.A. Bilmes, and W.S. Noble. Transmembrane topology and signal peptide prediction using dynamic bayesian networks. *PLoS Comput Biol* **4**, e1000213(2008).

18. L. Kall, A. Krogh, and E.L. Sonnhammer. Advantages of combined transmembrane topology and signal peptide prediction - the Phobius web server. *Nucleic Acids Res* **35**, W429-432 (2007).
19. T. Hirokawa, S. Boon-Chieng, and S. Mitaku. SOSUI: classification and secondary structure prediction system for membrane proteins. *Bioinformatics* **14**, 378-379 (1998).
20. D. Juretic, L. Zoranic, and D. Zucic. Basic charge clusters ad predictions of membrane protein topology. *J Chem Inf Comput* Sci **42**, 620-632 (2002).
21. Z. Yuan, J.S. Mattick, and R.D. Teasdale. SVMtm: Support vector machines to predict transmembrane segments. *J Comput Chem* **25**, 632-636 (2004).
22. A. Krogh, B. Larsson, G. von Heijne, and E.L. Sonnhammer. Predicting transmembrane protein topology with a hidden Markov model: Application to complete genomes. *J Mol Biol* **305**, 567-580 (2001).
23. K. Hofmann, and W. Stoffel. TMbase - A database of membrane spanning proteins segments. *Biol. Chem. Hoppe-Seyler* **374**, 166 (1993).
24. A. Bernsel, H. Viklund, A. Hennerdal, and A. Elofsson. TOPCONS: consensus prediction of membrane protein topology. *Nucleic Acids Res* **37**, W465-468 (2009).
25. M.G. Claros, and G. von Heijne. TopPred II: An Improved Software For Membrane Protein Structure Predictions. *CABIOS* **10**, 685-686 (1994).